Souillé, Fabien; Taccone, Florent; El Mertahi, Chaymae

A Multi-class Frazil Ice Model for Shallow Water Flows

A Multi-class Frazil Ice Model for Shallow Water Flows

Fabien Souillé, Florent Taccone
National Laboratory of Hydraulics and Environment
EDF R&D
6 Quai Watier, Chatou, France
Fabien.souille@edf.fr

Chaymae El Mertahi
EDF R&D and
ENSEEIHT
6 Quai Watier, Chatou, France
2 rue Charles Camichel, Toulouse, France

***Abstract*— Frazil ice, consisting of suspended disk shaped crystals, is the primary form of ice encountered in turbulent water bodies. Frazil ice clogging of power plants water intakes is a risk that companies have been challenged to address in recent years. In this context, physically based modelling is a useful tool that helps predict the evolution of water temperature and frazil ice during cold events. The TELEMAC-MASCARET system, with its recently introduced module KHIONE (coupled with TELEMAC-2D), allows to predict frazil ice dynamics via a thermal growth model, considering constant crystal radii. Among the drawbacks of this approach are the difficulty of choosing a representative radius and the turbulence variation not being taken into consideration in the thermal growth process. Multi-class models, assuming a discrete radius distribution, each class being composed of particles of the same radius, are more complex but provide a comprehensive description of frazil ice formation processes. This work is aimed at bringing state of the art frazil ice models into the TELEMAC-MASCARET system in order to expand its frazil modeling capabilities. A multi-class frazil ice model is therefore developed in the present work.**

Several processes are modelled to predict frazil ice formation and evolution: thermal growth and decay, consisting of phase change around crystals (increasing their size), is based on the heat transfer between turbulent water and frazil ice particles; secondary nucleation, which increases the number of nuclei, is caused by the fragmentation of particles due to collisions; flocculation, i.e. formation of larger aggregates, is assumed to be the net effect of flocculation and breakup processes; salinity is also taken into consideration as it has a significant impact on the fusion temperature. Thus, salt rejection process due to phase change is modelled as well.

The proposed model is able to simulate the evolution of depth-averaged temperature, salinity, frazil concentration in a 2D domain with time dependent atmospheric drivers. It has been confronted to laboratory experiments and is able to reproduce supercooling and temperature recovery for both fresh water and saline water under different turbulent conditions.

I. Introduction

When water temperature diminishes below the fusion point (supercooling), small particles of ice start to develop. These disk shaped crystals, known as frazil ice, are the primary form of ice encountered in turbulent water bodies. Their growth dynamic can lead to significant impact on environment and industrial facilities during cold events by accumulation on submerged structures such as water intake trash racks.

Frazil ice physics have been studied a lot over the last decades. A general overview can be found in [5, 8]. Several models are proposed in literature to predict the evolution of frazil concentration, temperature and ice cover during freeze-up periods like [23], [12], [22] or [15]. One has been added to TELEMAC-MASCARET v8p0 through a collaboration between EDF R&D, HR Wallingford and Clarkson University that gave birth to a new module dedicated to ice modelling named KHIONE [2] (coupled with TELEMAC-2D). It is based on the long experience acquired by Clarkson University with the development of river ice models such as CRISSP2D and DynaRICE [13, 22, 24]. However, the first implementation of KHIONE only incorporates tracer transport (Eulerian part of DynaRICE) and a static model for surface ice cover (static border ice). The focus of DynaRICE, i.e. ice cover dynamics developed in [13, 22] through an SPH formulation was not integrated into KHIONE by then. The frazil ice model in KHIONE relies on one equation to describe volume fraction, assuming all particles have the same radius, and the evolution of the concentration to be mainly governed by thermal growth [19, 22]. Turbulence variation is neglected in the model and a constant Nusselt number is considered.

The multi-class model developed in this study brings new processes to KHIONE, including thermal growth (and decay), secondary nucleation, flocculation, the effect of turbulence, salinity impact on fusion point and salt rejection. Its goal is to increase KHIONE's ability to predict frazil ice evolution in the early phase of supercooling. Frazil ice crystals vary in size from about 10^{-5} m to 10^{-3} m and can form large flocs up to 10^{-1} m [7]. Given the observed wide range of crystal radii in nature, and the sensitivity of a growth/melting model to this parameter, the use of the multi-class model provides a more physical representation of this process. Moreover, the multi-class approach allows to model a wide variety of physical processes which leads to a more comprehensive depiction of frazil crystals evolution in the flow. The multi-class description relies on a discrete distribution of radius, each class being composed of particles of the same radius. The evolution of the concentration of each class is then modelled with a set of advection-diffusion equations with source terms defined for each process. Thermal growth is based on the heat transfer between turbulent water and frazil ice crystals and consist of mass jumps between classes as proposed in [23]. However, the thermal growth model chosen in this study is the one later presented by [12] for its ability to model melting. Additionally, collisions between suspended frazil particles produce a fragmentation that creates new nuclei. This phenomenon, known as secondary nucleation, is modelled as

proposed in [20]. Collisions also produce flocculation and breakup and the formation of larger aggregates is assumed to be the net effect of these processes as suggested in [20]. Turbulence also plays an important role in the effectiveness of the heat transfer between water and the particle, and consequently in frazil ice formation as it increases thermal growth rate. It also plays a key role in estimating the collision rate between particles [8, 11, 20]. Two options are proposed in this model to estimate turbulent parameters, a k-ε model and a simplified depth integration of vertical k-ε profiles as proposed in [23]. Finally, salinity has a significant impact on frazil ice since it diminishes the fusion point. Additionally, frazil formation releases salt, increasing the local salinity. Both impact on the freezing temperature and salt rejection process are modelled in this study.

Frazil ice formation has been studied in laboratory experiments [3, 4, 10, 18] at relatively small scale. Understanding the formation of frazil in large water bodies is still challenging and is an active research topic. Some attempts to measure frazil in nature have been made as in [21]. Frazil ice concentration being the focus of our study, it has been decided to assess KHIONE's validity in the supercooling phase. The model proposed in this study is therefore confronted to experimental data from [3] for fresh water and [10] for saline water in the case of a turbulent flow in a racetrack configuration.

This paper is organised as followed. First, the model equations and numerical resolution method are presented. Then, it is confronted to experimental data [3, 10] to evaluate its representation of the temperature and frazil ice evolution. Finally, the performances and limitations of the model are discussed.

II. Model Formulation

This study is focused on environmental flows in rivers, lakes or coastal areas. The 2D viscous Shallow Water Equations (SWE) are considered for the mean flow, and are introduced hereafter. Temperature, salinity and frazil volume fraction are considered to be passive scalars and are modelled with convection-diffusion equations with source terms. Frazil volume fraction is assumed small compared to 1 so that it does not affect water density nor viscosity. Ice cover dynamics are not taken into account in the model.

A. Hydrodynamics

The SWE can be obtained from the incompressible Navier-Stokes equations for a Newtonian fluid, assuming that the water depth h is small compared to the longitudinal length of the domain. The conservation of mass and momentum reads:

$$\frac{\partial h}{\partial t} + \nabla.(h\mathbf{u}) = 0, \tag{1}$$

and

$$\frac{\partial h\mathbf{u}}{\partial t} + \nabla.\left(h\mathbf{u}\otimes\mathbf{u} + g\frac{h^2}{2}\mathbf{I}\right) = -gh\nabla z_b + \nabla.(h\mathbf{D}) - \frac{\boldsymbol{\tau}_b}{\rho}. \tag{2}$$

The unknowns of the system are the depth averaged mean velocity $\mathbf{u} = [u(x,y,t), v(x,y,t)]^{\boldsymbol{T}}$ and the water depth $h(x,y,t)$. The space and time coordinates denoted (x,y) and t will be dropped in the following for clarity's sake. In Equations (1) and (2) z_b is the bottom elevation, $\boldsymbol{\tau}_b$ is the bottom shear stress, g is the gravitational acceleration and ρ is the density of water, assumed to be constant. The diffusion tensor $\mathbf{D}$ is written as $\mathbf{D} = 2(\nu + \nu_t)\boldsymbol{\varepsilon}$ where $\boldsymbol{\varepsilon} = \frac{1}{2}(\nabla\mathbf{u} + \nabla\mathbf{u}^T)$ is the rate of strain tensor, ν the kinetic viscosity of water and ν_t the turbulent viscosity. Equations (1) and (2) need closure relations for the bottom shear stress and the turbulent viscosity. The Manning-Strickler relation is used for bottom shear stress and either a k-ε or a constant viscosity model is used for the estimation of ν_t.

B. Frazil evolution

A discrete radius distribution is used to describe suspended frazil ice. A number of N_C classes are considered. The balance equation of the frazil volume fraction for the k^{th} class is given by:

$$\frac{\partial C_k}{\partial t} + \mathbf{u}.\nabla C_k = \nabla.\left(\nu_{t,k}\nabla C_k\right) + S_{GM}^k + S_{SN}^k + S_{FB}^k, \tag{3}$$

where C_k is the depth averaged volume fraction and $\nu_{t,k}$ is the turbulent diffusivity of the k^{th} frazil class. The source terms S_{GM}^k, S_{SN}^k, S_{FB}^k stand for thermal growth (melting), secondary nucleation and flocculation (breakup) respectively. The total frazil concentration C can be computed as $C = \sum_{k=1}^{N_C} C_k$. The number of particles per unit volume for each class is given by $N_k = C_k/V_k$ with V_k the frazil crystal volume of class k.

1) Thermal growth

Let us first introduce the heat flux between frazil crystals of class k and water in Equation (4):

$$q_k = \frac{K_w Nu_k}{l_k}(T_i - T), \tag{4}$$

where K_w is the thermal conductivity of water and T_i the crystal temperature assumed to be equal to the freezing temperature $T_f(S)$ which depends on the salinity S such that $T_f(S) = -0.0575S + 0.00171S^{3/2} - 0.00021S^2$. Frazil crystals are supposed to have the same disk shaped geometry characterized by a radius r_k and a thickness e_k, related with a constant ratio R such that $e_k = 2r_k/R$. R is fixed to 8 based on [8]. The characteristic length scale l_k for the crystals of class k is supposed to be equal to r_k as suggested in [11, 12]. The Nusselt number Nu_k is defined with the parametrization initially proposed in [1] and [25] and summarized in [5] and [11]. Let us define the ratio $m^* = r_k/\eta$ between the radius and the Kolmogorov length scale noted η and defined by:

$$\eta = \left(\frac{\nu^3}{\varepsilon}\right)^{1/4}, \tag{5}$$

where ε is the turbulent kinetic energy dissipation rate and ν the molecular viscosity of the fluid. For small particles, heat transfer is governed by diffusion and convection, and the Nusselt number can therefore be written in Equation [6].

$$Nu_k = \begin{cases} 1 + 0.17 m_k^* P_r^{1/2} & \text{if } m_k^* \le P_r^{-1/2} \\ 1 + 0.55 m_k^{*2/3} P_r^{1/3} & \text{if } P_r^{-1/2} < m_k^* \le 10 \end{cases}. \tag{6}$$

For larger particles ($m_k^* > 1$), heat transfer is governed by turbulent mixing of the boundary layer around the crystal and the Nusselt number is defined by

$$Nu_k = \begin{cases} 1.1 + 0.77\alpha_T^{0.035} m_k^{*\,2/3} P_r^{1/3} \text{ if } \alpha_T m_k^{*4/3} \leq 1000 \\ 1.1 + 0.77\alpha_T^{0.25} m_k^{*} P_r^{1/3} \text{ if } \alpha_T m_k^{*4/3} > 1000 \end{cases}, \quad (8)$$

in which P_r denotes the Prandlt number, defined as the ratio between molecular and thermal diffusivity, and $\alpha_T = \frac{\sqrt{2k}}{|\mathbf{u}|}$ the turbulent intensity.

The thermal growth (or decay) source term S_{GM}^k represents the net rate of volume change of class k resulting from interactions with classes $k-1$ and $k+1$ due to freezing or melting. Following [23] for thermal growth and [12] for the introduction of melting, the net rate of volume fraction change for the frazil class k can be defined as:

$$S_{GM}^k = \frac{V_k}{\Delta V_{k-1}}[(1-H)M_k + HG_{k-1}] - \frac{V_k}{\Delta V_k}[(1-H)M_{k+1} + HG_k], \quad (10)$$

with $H = He(T_f - T)$, where He is the Heaviside function and V_k the volume of ice crystals. Volume ratios $\Delta V_k = V_{k+1} - V_k$ account for the scaling of the computed volume change to the number of particles that jump from a class to another. As explained in [8], frazil crystals are supposed to grow only from their edges because of their disk shape, which leads to the production rate for thermal growth defined by:

$$G_k = \frac{K_w Nu_k}{L_i \rho_i}(T_f - T)\frac{2}{r_k^2} C_k, \quad (11)$$

whereas the melting is supposed to occur on all surfaces of the disk which leads to:

$$M_k = \frac{K_w Nu_k}{L_i \rho_i}(T_f - T)\frac{2}{r_k}\left(\frac{1}{r_k} + \frac{1}{e_k}\right) C_k, \quad (12)$$

where ρ_i=916.8 kg.m^{-3} is the ice density and L_i=3.35$\cdot 10^5$ J.kg^{-1} the latent heat of ice fusion. For the first and last classes, the boundary conditions $V_0 = V_{N_c+1} = G_0 = G_{N_c} = M_{N_c+1} = 0$ are used [12].

When only one class of frazil is selected in KHIONE, the model uses a monoclass frazil ice model, in which only thermal growth is considered. In this case, the source term for frazil ice is defined by:

$$S_{GM}^1 = (1-H)M_1 + HG_1. \quad (13)$$

2) Secondary nucleation

When frazil crystals collide, new nuclei are detached which increases the volume fraction of the smallest particles. This is known as the secondary nucleation process. Secondary nucleation can be modelled using an approximation of the collision frequency between particles [20]. A particle with a velocity w_k^r relative to the fluid sweeps a volume $\delta V = w_k^r \pi r_k^2 \delta t$ during δt. The collision frequency can be estimated as $f_{coll}^k \sim \tilde{n}\delta V n_k/\delta t$, in which $\tilde{n}$ is an estimation of the average number of particles per unit volume, defined in Equation (14) and n_k the number of particles of class k per unit volume:

$$\tilde{n} = \max\left(\sum_{j=1}^{N_c} n_j, n_{max}\right). \quad (14)$$

n_{max} is a calibration parameter used to limit collisions impact. The relative velocity is estimated from the rising and turbulent velocities such that

$$w_k^r = \sqrt{{U_k^t}^2 + w_k^2}, \quad (15)$$

with $U_k^t = 2r_k\sqrt{\frac{\varepsilon}{15\nu}}$ and w_k the buoyant rise velocity of frazil crystals. Different empirical approaches are proposed in the literature to estimate w_k, i.e. [16], [9] and [5]. In this study, we use the formulation proposed in [9] which has been confronted to lab and field data. The rise velocity is estimated with:

$$w_k = \sqrt{\frac{2ge_k(\rho - \rho_i)}{C_d \rho}}. \quad (16)$$

in which the drag coefficient C_d can be calculated with the Reynolds number of frazil crystals as described in [9]. Finally, volume fraction change rate due to secondary nucleation can be written as:

$$S_{SN}^k = \begin{cases} \sum_{j=2}^{N} \pi\tilde{n} w_j^r r_j^2 C_j \text{ if } k = 1 \\ -\pi\tilde{n} w_k^r r_k^2 C_k \text{ if } k \neq 1 \end{cases}. \quad (17)$$

3) Flocculation

Flocculation and breakup are supposed to result only in a net increase in scales [20]. The effectiveness of class jumps is supposed to be linearly dependent on radius:

$$\beta_k = a_{floc}\frac{r_k}{r_1}, \quad (18)$$

where a_{floc} represents the proportion of frazil crystals that move from class k to $k+1$ per second. A value of a_{floc} =10^{-4} s^{-1} is suggested in [20] based on a size distribution spectrum. This value depends on turbulence as discussed hereafter. The flocculation source term is defined as:

$$S_{FB}^k = \beta_{k-1} C_{k-1} - \beta_k C_k. \quad (19)$$

C. Thermal balance

The water fraction of the water-ice mixture is characterized by a temperature, subject to a heat balance defined as:

$$\frac{\partial}{\partial t}[(1-C)T] + \nabla.[(1-C)\mathbf{u}T] = \nabla.(\nu_t \nabla[(1-C)T]) + \frac{\phi}{h\rho c_p} - \frac{S_L}{\rho c_p}, \quad (20)$$

with c_p= 4.1855$\cdot 10^3$ J.kg^{-1}.K^{-1} the specific heat of water and ϕ the net heat flux at the free surface in W.m^{-2}. The heat source S_L due to melting or freezing, can be written as $S_L = \rho L_i \delta w - \rho c_p T_i \delta w$, expressed in W.m^{-3}, where T_i the crystal temperature, assumed to be equal to the freezing temperature and δw is the water volume change rate (s^{-1}) due to frazil ice evolution expressed as:

$$\delta w = -\frac{\rho_i}{\rho}\sum_{k=1}^{N_c} S_{GM}^k. \quad (21)$$

Equation (20) can be developed as:

$$(1-C)\frac{\partial T}{\partial t} + (1-C)\mathbf{u}.\nabla T = (1-C)\nabla.(\nu_t \nabla T) - 2\nu_t \nabla T \nabla C + \frac{\phi}{h\rho c_p} - \delta w\left(T - T_f + \frac{L_i}{c_p}\right), \quad (22)$$

Additionally, the term $2\nu_t \nabla T \nabla C$ in Equation (22) can be neglected after [12], considering the hypothesis $C \ll 1$. Hence, the following heat balance equation is obtained:

$$\frac{\partial T}{\partial t} + \mathbf{u}.\nabla T = \nabla.(\nu_t \nabla T) + \frac{\phi}{h\rho c_p (1-C)} + \frac{\rho_i}{\rho(1-C)}\left(T - T_f + \frac{L_i}{c_p}\right)\sum_{k=1}^{N_c} S_{GM}^k. \quad (23)$$

Equation (23) can be further simplified by considering $C \ll 1$ and $T - T_f \ll \frac{L_i}{c_p}$, which leads to:

$$\frac{\partial T}{\partial t} + \mathbf{u}.\nabla T = \nabla.(\nu_t \nabla T) + \frac{\phi}{h\rho c_p} + \frac{\rho_i L_i}{\rho c_p}\sum_{k=1}^{N_c} S_{GM}^k. \quad (24)$$

Both Equations (23) and (24) were implemented in KHIONE in this study.

D. Salinity balance

The salinity balance is given by:

$$\frac{\partial S}{\partial t} + \mathbf{u}.\nabla S = \nabla.\left(\nu_{t,S}\nabla S\right) + S_R, \quad (25)$$

in which $\nu_{t,S}$ is the turbulent diffusivity and S_R is the salt rejection source term. Salt rejection was taken into account in the single class model developed in [19]. In the case of multiple classes, salt rejection can be expressed as a function of the water phase rate of volume change δw. Finally, the salinity rejection source can be calculated as:

$$S_R = \frac{\rho_i}{\rho}(S - S_i)\sum_{k=1}^{N_c} S_{GM}^k, \quad (26)$$

with S_i the salinity of frazil crystals assumed to be equal to zero.

E. Turbulence

Turbulence parameters, required to compute the different source terms above defined, are estimated using the k-ε solver from TELEMAC-2D. A second option, suggested in [23], has been implemented to reduce computational cost for simple applications and relies on a depth integration of k and ε profiles defined as:

$$k(z) = \frac{u_*^2}{\sqrt{C_\mu}}\left(1 - \frac{z}{h}\right), \quad (27)$$

$$\varepsilon(z) = \frac{u_*^3}{kz}\left(1 - \frac{z}{h}\right), \quad (28)$$

in which u_* is the friction velocity and $C_\mu = 0.09$. The profiles are integrated between the upper bound of the viscous boundary layer and the free surface [23]. Turbulent viscosities are then computed as $\nu_t = C_\mu k^2/\varepsilon$.

F. Numerical resolution

1) Time integration

Time integration of Equations (3), (24) and (25) is done with a time splitting technique. First, the convection-diffusion operators are solved using classical numerical schemes available in TELEMAC-2D. Let us note C_k^{n+1} the volume fraction of frazil and T^{n+1} the temperature at time t^{n+1}. The fields obtained after the first step are noted $\tilde{C}_k$ and $\tilde{T}$. Time integration of source terms is then done as:

$$\begin{cases} C_k^{n+1} = \tilde{C}_k + \Delta t^n\left(S_{GM}^{k,1} + S_{SN}^k + S_{FB}^k\right) \quad \forall k \in [\![1, N_c]\!] \\ T^{n+1} = \tilde{T} + \Delta t^n\left(\frac{\phi}{h\rho c_p} + \frac{\rho_i}{\rho}\frac{L_i}{c_p}\sum_{k=1}^{N_c} S_{GM}^{k,2}\right) \end{cases}, \quad (29)$$

with Δt^n the time step and $S_{GM}^{k,1}$ and $S_{GM}^{k,2}$ defined by:

$$S_{GM}^{k,1} = \left(T_f^n - T^n\right)\left(\frac{V_k}{\Delta V_{k-1}}[(1-H^n)\chi_k^n C_k^* + H^n\psi_{k-1}^n C_{k-1}^n] - \frac{V_k}{\Delta V_k}[(1-H^n)\chi_{k+1}^n C_{k+1}^n + H^n\psi_k^n C_k^*]\right), \quad (30)$$

$$S_{GM}^{k,2} = \left(T_f^n - T^*\right)\left(\frac{V_k}{\Delta V_{k-1}}[(1-H^n)\chi_k^n C_k^n + H^n\psi_{k-1}^n C_{k-1}^n] - \frac{V_k}{\Delta V_k}[(1-H^n)\chi_{k+1}^n C_{k+1}^n + H^n\psi_k^n C_k^n]\right), \quad (31)$$

in which ψ_k^n and χ_k^n are defined with:

$$\psi_k^n = \frac{2K_w Nu_k^n}{\rho_i L_i r_k^2}, \quad (32)$$

$$\chi_k^n = \frac{2K_w Nu_k^n}{\rho_i L_i r_k}\left(\frac{1}{r_k} + \frac{1}{e_k}\right). \quad (33)$$

Replacing $*$ by n in Equations (30) and (31), the Euler explicit scheme is obtained and $S_{GM}^{k,1} = S_{GM}^{k,2}$. A semi-implicit scheme is obtained replacing $*$ by $n+1$ in Equations (30) and (31). The resolution is subject to time step constraints with both approaches. Note that both secondary nucleation and flocculation have been treated explicitly in this work. A semi-implicit approach similar to the one described for thermal growth is possible, but has not been tested yet. Finally, no fully implicit time scheme has been presented in this study, as it would need an overall modification of KHIONE's structure, which was out of the scope of this work.

2) Stability and positivity of frazil volume fraction

For a single class of frazil in case of supercooling ($T < T_f$), the numerical scheme defined in Equation (29) becomes:

$$\begin{cases} C^{n+1} = \tilde{C} + \Delta t^n \psi_1^n (T_f^n - T^n) C^* \\ T^{n+1} = \tilde{T} + \Delta t^n \frac{\phi^n}{h\rho c_p} + \Delta t^n \frac{\rho_i}{\rho}\frac{L_i}{c_p}\psi_1^n (T_f^n - T^*) C^n \end{cases}. \quad (34)$$

Neglecting advection-diffusion and supposing $T_f = 0$, the stability of the system and the positivity of C, in the case of the Euler explicit time scheme, lead to a constraint on time step defined by:

$$\Delta t^n \leq \min\left(2/\left[\frac{\rho_i}{\rho}\frac{L_i}{c_p}\psi_1^n C^n + \frac{\phi^n}{h\rho c_p|T^n|}\right], \frac{1}{\psi_1^n|T^n|}\right). \quad (35)$$

This constraint implies that the time step Δt^n at time t^n, should be sufficiently small with respect to a coefficient that is proportional to the squared radius of frazil crystals (due to the definition of ψ_1^n).

In theory, the condition (35) is no longer valid for the numerical scheme defined in Equation (29), and the stability condition of this scheme is yet to be determined. However, numerical tests suggest that the radius of the smallest class is still the main limiting factor. In the numerical simulations presented hereafter, the time step has been adjusted to verify the stability condition and the convergence of the results.

3) *Maximum concentration*

A limiter is introduced for both mono-class and multi-class models to prevent the concentration from reaching the maximum allowed volume fraction. This limiter is mandatory since the concentration linearly increases at constant cooling rate. When concentration reaches a threshold of 1, all sources are frozen and only melting is authorized.

III. APPLICATION

A. *Calibration*

The model presented in this study has two main calibration parameters, namely n_{max} and a_{floc} respectively from Equations (14) and (18). Additionally, one has to provide a distribution of radius and initial seeding in order to run the model. In this section, the calibration method, based on previous work in the literature [20, 26] is described.

A typical distribution of radii observed in experiments is the lognormal distribution [4, 6]. Such distribution has also been recently observed in Alberta Rivers as shown in [14]. Given the difficulty of providing correct parameters for the lognormal distribution, authors often use a simplified distribution of particles, introduced in [17]. As for the radii, they typically range from 4 µm to 5 mm [4, 17]. In this study, radius for each classes are spread out uniformly between minimum and maximum radius which are set to 10 µm to 1 mm respectively, with a default number of classes set to 10, which gives the best compromise between precision and computational cost.

Modelling seeding and primary nucleation is still a major difficulty in frazil studies as the seeding process is not fully understood yet. It depends on atmospheric conditions (snow, mist) and water impurities, which may considerably vary in the different experiments and in nature. Furthermore, frazil artificial seeding is carried out in experiments as in [10], which consists in releasing ice scraps in water at a controlled rate. In this study, the initial seeding is done by introducing a number of particle, noted N_0, supposed to be equally shared by all classes [20]. In order for the model to be able to properly model multiple growth and melting sequences, a minimum threshold of concentration, based on N_0 is set. Below this threshold, all processes are disabled except thermal growth.

Parameters n_{max} and a_{floc} influence the evolution of particles distribution in time. The parameter a_{floc} is fixed to 10^{-4} as suggested in [20]. This reduces the number of calibration parameters to two, n_{max} and N_0. Besides, [20] propose to set a common value of n_{max} for all experiences. Therefore, only N_0 needs to be chosen specifically for each case. However, it has been shown in [26] that a common parameter n_{max} for all experiments is difficult to choose as it depends on turbulence. Correlations between n_{max}, N_0 and turbulent intensity, based on numerical simulations, have been proposed in [26] to overcome this difficulty. The presence of such correlations between the parameters suggests that calibrating them independently, as in [20], might not be optimal. Further investigations, for example using data assimilation methods, should be considered but are out of the scope of this paper. Consequently, the values proposed in [20] are used as a first guess, and then both parameters n_{max} and N_0 are adjusted for each experiment.

B. *Carstens experiments*

Carstens experiments [3] were conducted in a recirculating oval flume of 600 cm long, 30 cm deep and 20 cm wide. Water depth was set to 20 cm and temperature was recorded at approximately 5 to 10 cm deep with a mercury thermometer marked to 0.01 °C. The physical parameters of the experiment are summed up in the Table 1. Following the calibration method previously introduced, numerical simulations were carried out with a time step of 0.1 s. The evolution of temperature and total frazil volume fraction are presented in Figure 1. The characteristic time t_c corresponds to the moment when 90% of the maximum temperature depression is recovered. The calibrated parameters are presented in Table 2. Additionally, the evolution of frazil distribution is presented in Figure 2 for the first Carstens experiment.

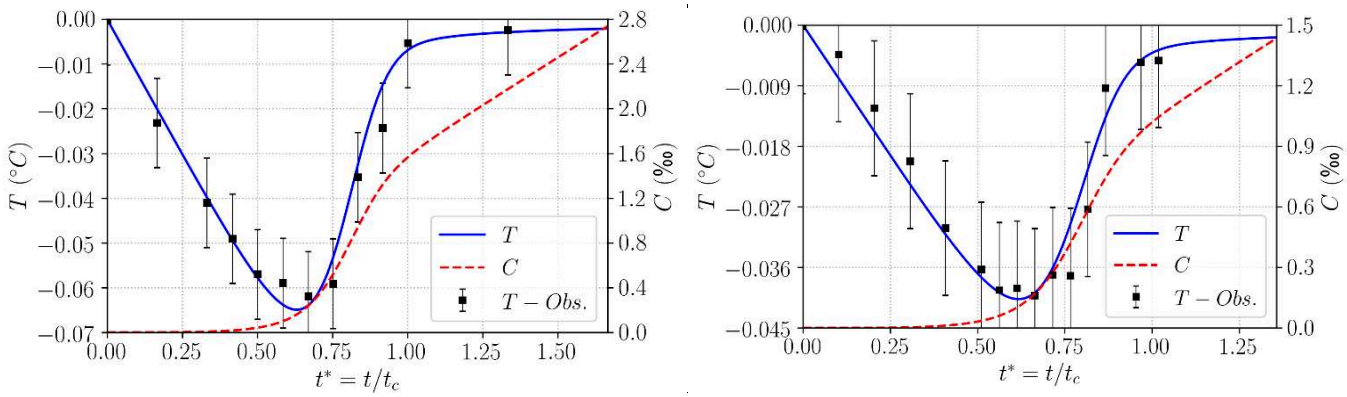

Figure 1: Simulated temperature and total frazil volume fraction with comparison to Carstens experiments I (left) and II (right).

TABLE 1: PHYSICAL PARAMETERS OF EXPERIMENTS

Case	h (m)	u (m/s)	ϕ/h (W/m³)	S (ppt)	k (m²/s²)	ε (m²/s³)
Carstens I	0.2	0.5	1400	0	$9.6\cdot 10^{-4}$	$1.2\cdot 10^{-3}$
Carstens II	0.2	0.5	550	0	$4.8\cdot 10^{-4}$	$3.8\cdot 10^{-4}$
Tsang & Hanley	0.11	0.15	122	29-31	-	-

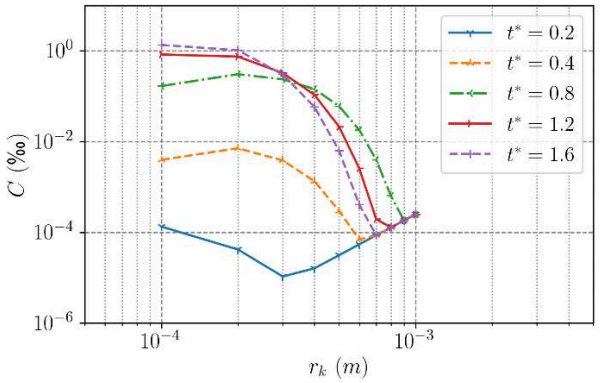

Figure 2: Evolution of simulated frazil volume fraction per class in the first Carstens experiment.

TABLE 2: CALIBRATED PARAMETERS.

Case	a_{floc} (s⁻¹)	n_{max}	N_0 (m⁻³)
Carstens I	10^{-4}	$1\cdot 10^{6}$	$3.2\cdot 10^{2}$
Carstens II	10^{-4}	$1.5\cdot 10^{6}$	$1.9\cdot 10^{2}$
Tsang & Hanley	10^{-4}	$2\cdot 10^{6}$	$2\cdot 10^{3}$

C. Tsang and Hanley experiments

Tsang & Hanley experiments [10] (C) were conducted in a recirculating, racetrack shaped, flume of 65 cm long, 13 cm deep and 15 cm wide. The tank was filled with sea-water of salinity comprised between 29 and 31 ppt. The frazil concentration was estimated using temperature measurements, made with a thermometer calibrated to 0.0001 °C, with repeatability of 0.001 °C. This leads to an absolute error of $1.25\cdot 10^{-5}$ on frazil observations. The physical parameters of the experiment are summed up in Table 1. To reproduce experiments, a momentum source term is introduced to simulate the propeller. The source term is adjusted in order to reach a hydrodynamic steady state with a mean flow velocity of 0.15 m·s^{-1}. The Manning friction law is used with friction factor of 0.011 m$^{-1/3}$·s. Turbulent parameters were estimated with Equations (27) and (28) giving average values of k=$7\cdot 10^{-6}$ m²·s^{-2} and ε=$2.4\cdot 10^{-6}$ m²·s^{-3} in the racetrack at steady state. Figure 3 illustrates the configuration of the model and steady state mean flow velocity.

Artificial seeding described in [10] was reproduced by introducing a total number of particles N_0 when temperature reaches the seeding temperature, denoted T_n. The salinity was set to 31.2 ppt for all simulations, giving a fusion temperature of T_f=−1.7056 °C. Common calibration parameters were adjusted to the nine experiments, as shown in Table 2. Results are presented in Figure 6 with $C^* = C/C_c$, the characteristic total frazil concentration being defined by $C_c = C(t_c)$.

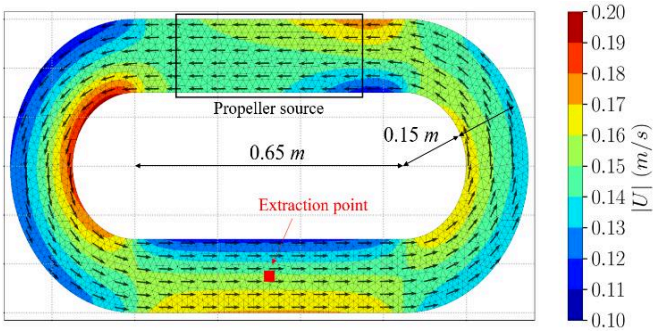

Figure 3: Racetrack geometry used in Tsang & Hanley experiments (1985) and simulated hydrodynamic steady state.

D. Sensitivity to model parameters

A sensitivity analysis is carried out on different parameters of the model. The sensitivity to the initial seeding N_0 and the maximal number of collision for secondary nucleation n_{max} are presented in Figure 4 and 5 respectively.

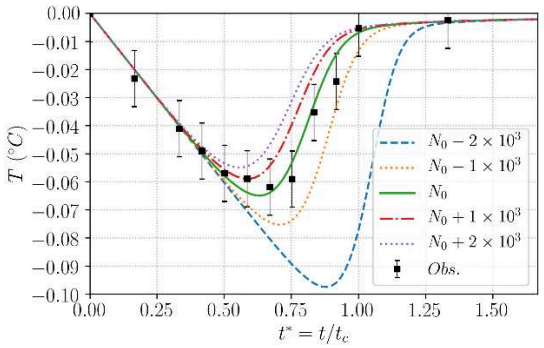

Figure 4: Sensitivity to the initial seeding for the first Carstens experiment.

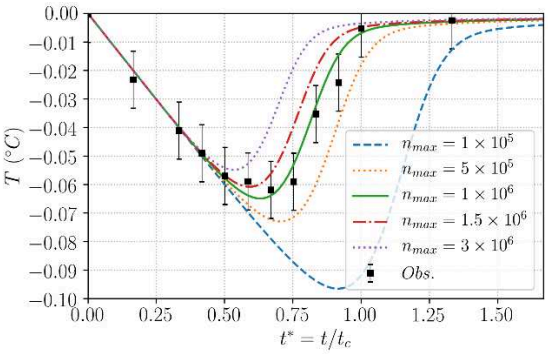

Figure 5: Sensitivity to n_{max} *for the first Carstens experiment.*

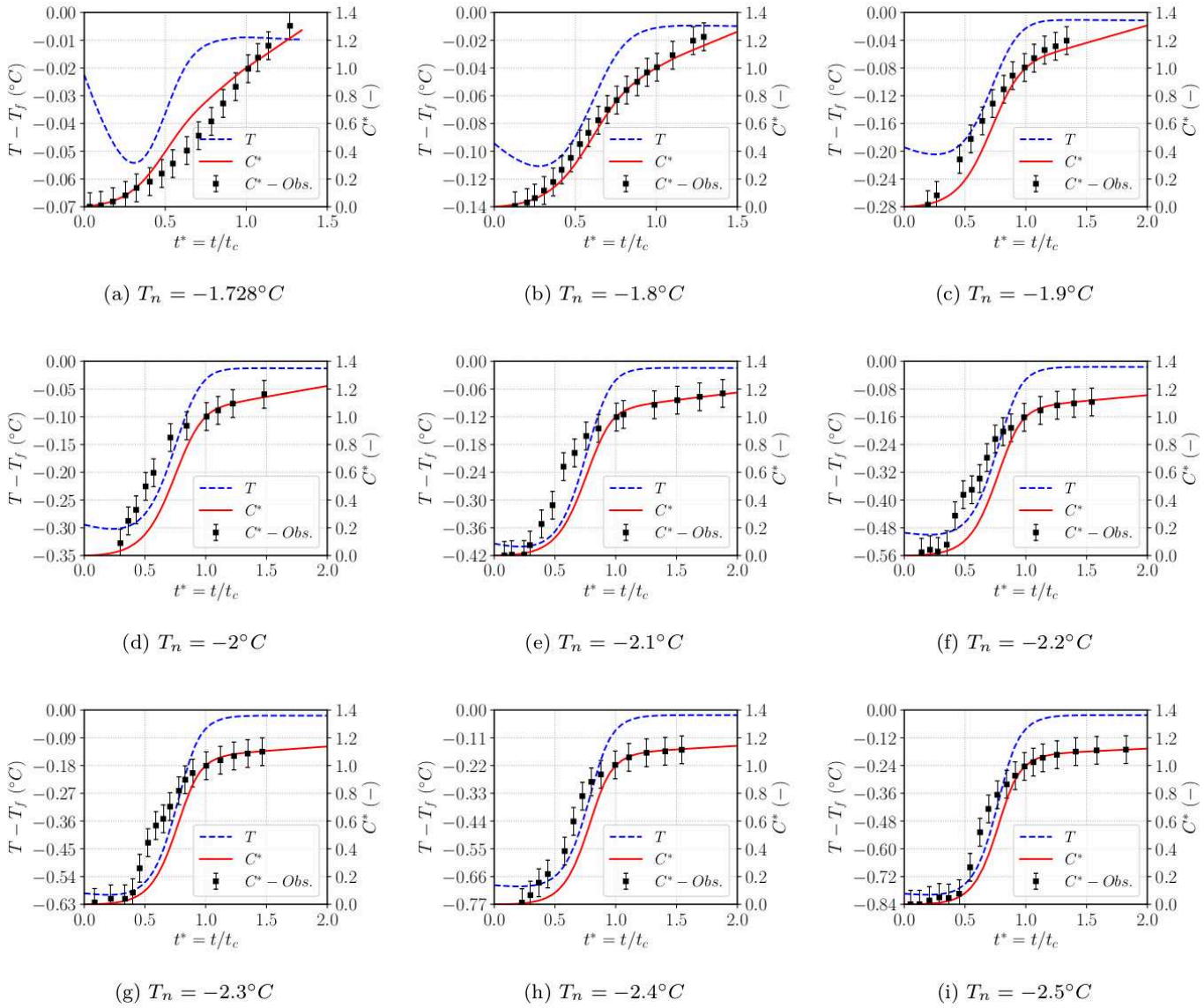

Figure 6: Simulated temperature and normalized total frazil volume fraction with comparison to Tsang & Hanley experiments for different seeding temperatures.

IV. Discussion

The confrontation of numerical results to experimental data is encouraging as the model is able to reproduce supercooling and temperature recovery under different turbulent and salinity conditions as shown on Figure 1 and Figure 6.

The sensitivity analysis results indicate that small modifications of N_0 and n_{max} have significant impact on the results. Consequently, fitting temperature or total frazil concentration may be tedious and should be done precautiously. In addition to global evolution of frazil total concentration and temperature, one has to verify the evolution of the particles' distribution against time. Unfortunately, frazil ice distribution have not been measured in Carstens and Tsang & Hanley experiments. However, distributions obtained in [4] and later used in [26] to calibrate a multi-class model, indicates that a n_{max} of 10^6 combined with an initial seeding of $6.4 \cdot 10^3$ allow a good representation of frazil distribution evolution against time. This is not the case with the present work as shown in Figure 2. The evolution of simulated distribution with $n_{max} = 10^6$ indicates a predominance of secondary nucleation over thermal growth and flocculation, leading to higher concentration on the lower classes. This causes the model to miss the expected lognormal distribution of particles observed in [4] even though a good match is obtained on total frazil concentration and temperature. Such a difference between the results obtained in this work and [26] might come from the overestimation of thermal growth, for which the correction presented in [11] is taken into account in the present work. Other probable causes are the model chosen for the estimation of the rise velocity and the gravitational removal that is neglected in present study. Consequently, additional tuning of model parameters is required to expect a good representation of frazil ice distribution against time with the current model. Furthermore, the model convergence in terms of number of classes still needs to be studied, as well as its sensitivity to the initial conditions. For this purpose, a comprehensive sensitivity analysis should be

considered in the future. Optimal calibration methods could also provide insight on the best way to fit parameters for the present model.

The TELEMAC-MASCARET system is best suited for large-scale environmental modelling. However, the experiments reproduced in the present work were conducted on small-scale geometries of less than several meters. Despite the lack of frazil ice data in natural water bodies, additional validation on larger domains should nonetheless be considered in the future to assess the applicability of the model on large-scale geometries.

The present model has been developed in the shallow water framework, specifically for coupling with TELEMAC-2D. It should be mentioned that the shallow water assumption does not allow to describe the vertical profile of frazil concentration. This may have a significant impact in real applications where the flow is not vertically mixed and thermohaline stratification is well established. The impact would be a higher frazil concentration close to the free surface, where temperature and salinity are low. Furthermore, a 3D model would allow a better representation of the buoyancy of frazil crystals, hence increasing the vertical heterogeneity of frazil volume fraction.

V. Conclusion

In this study, a multi-class model for frazil ice modelling has been developed for TELEMAC-2D/KHIONE. This work brings state of the art frazil ice model into KHIONE expanding its capabilities and allowing more advanced investigation of frazil ice processes in shallow water flows. Several processes have been implemented, including thermal growth, secondary nucleation and flocculation. Turbulence has been taken into account in the processes by a coupling with TELEMAC-2D k − ε solver. Salinity has also been taken into account by means of a variable fusion temperature and a salt rejection source term. Euler explicit and semi-implicit time schemes were presented for the resolution of the coupled system. The model has been validated on two experiments from literature, one with fresh water and the other with ocean water.

The depth averaged temperature and total frazil volume fraction evolution obtained with the calibrated model are in good accordance with experimental data for both fresh and saline water. However, the model is sensitive to the calibration parameters (maximal collision number for secondary nucleation and initial seeding) which does not allow a good representation of the typical lognormal distribution of particles with standard values suggested in literature. Further investigations on the impact of each process are needed to obtain a better understanding of these parameters influence on particles' distribution. Additionally, a comprehensive sensitivity analysis would be useful in order to better describe the capabilities and limitations of the present model.

References

[1] G. K. Batchelor. Mass transfer from small particles suspended in turbulent fluid. Journal of Fluid Mechanics, 98(3):609–623, 1980.

[2] S. E. Bourban, H. F., H. T. Shen, and R. Ata. Introducting khione - (eulerian) part i of the ice modelling component of telemac. TUC, 2018.

[3] T. Carstens. Experiments with supercooling and ice formation in flowing water. Geofys. Publ. Norway, 26(9) (3-18), 1966.

[4] S. Clark and J. Doering. Laboratory experiments on frazil-size characteristics in a counterrotating flume. Journal of Hydraulic Engineering, 132:94–101, 2006.

[5] S. F. Daly. Frazil ice dynamics. CRREL Monograph 84-1, 1984.

[6] S. F. Daly. Frazil ice measurement in crrel's flume facility. IAHR Ice Symp., Iowa City, page 427–438, 1986.

[7] S. F. Daly. Frazil ice blockage of intake trash racks, cold regions technical digest no. 91-1. Technical report, US Army Corps of Engineers, 1991.

[8] S. F. Daly. Report on frazil ice. Technical report, International Association for Hydraulic Research, Working Group on Thermal Regimes, Special Report 94-23, 1994.

[9] J. Gosink and T. Osterkamp. Measurements and analyses of velocity profiles and frazil ice-crystal rise velocities during periods of frazil-ice formation in rivers. Annals of Glaciology, 4:79–84, 1983.

[10] T. O. Hanley and G. Tsang. Formation and properties of frazil in saline water. Cold Regions Science and Technology, 8:209–221, 1984.

[11] P. Holland, D. L. Feltham, and S. F. Daly. On the nusselt number for frazil ice growth—a correction to "frazil evolution in channels" by lars hammar and hung-tao shen. Journal of Hydraulic Research, page pp. 1–4, 2006.

[12] P. R. Holland and D. L. Feltham. Frazil dynamics and precipitation in a water column with depth-dependent supercooling. Journal of Fluid Mechanics, 530:101–124., 2005.

[13] L. Liu and H. T. Li, H. andShen. A two-dimensional comprehensive river ice model. 18th IAHR International Symposium on Ice, 2006.

[14] V. MacFarlane, M. Loewen, and F. Hicks. Measurements of the size distribution of frazil ice particles in three alberta rivers. Cold Regions Science and Technology, 2017. doi: 10.1016/j.coldregions.2017.08.001.

[15] Z.-y. Mao, J. Yuan, J. Bao, X.-f. Peng, and G.-q. Tang. Comprehensive two-dimensional river ice model based on boundary-fitted coordinate transformation method. Water Science and Engineering, 7(1):90–105, 2014.

[16] V. Matoušek. Frazil and skim ice formation in rivers. In Proceedings of the IAHR Ice Symposium, 1992.

[17] R. Mercier. The reactive transport of suspended particles: Mechanics and modeling. PhD thesis, Joint Committee on Oceanographic Engineering, Massachusetts Institute of Technology, Cambridge, Mass., 1984.

[18] B. Michel. Theory of formation and deposit of frazil ice. Eastern Snow Conference, Proc. Annual Meeting, Quebec., 1963.

[19] A. Omstedt. On supercooling and ice formation in turbulent sea-water. Journal of Glaciology, 31(109), 1985.

[20] A. Omstedt. Simulation of supercooling and size distribution in frazil ice dynamics. Cold regions science and technology, 1994.

[21] M. Richard. Field Investigation of Freshwater Frazil Ice Dynamics. PhD thesis, Faculté des études supérieures de l'Université Laval, 2011.

[22] H. T. Shen. Mathematical modeling of river ice processes. Cold Regions Science and Technology, 62 (1):pp.3–13, 2010. doi: doi:10.1016/j.coldregions.2010.02.007.

[23] H. T. Shen and L. Hammar. Frazil evolution in channels. Journal of Hydraulic Research, 2010. doi: 10.1080/00221689509498572.

[24] H. T. Shen and A. M. Wasantha Lal. A mathematical model for river ice processes. Technical report, US Army Corps of Engineers Cold Regions Research and Engineering Laboratory, 1993.

[25] P. H. Wadia. Mass transfer from spheres and discs in turbulent agitated vessels. PhD thesis, Department of Chemical Engineering, Massachusetts Institute of Technology, Cambridge, MA., 1974.

[26] S. M. Wang and J. C. Doering. Numerical simulation of supercooling process and frazil ice evolution. Journal of Hydraulic Engineering, 2005.